

Cooling Performance Design for Super Motor and Its Experimental Validation

Naruhiko Tan*

Minoru Arimitsu *

Yuji Naruse*

Jun Watanabe*

This paper describes the development of a cooling system for the Super Motor and its experimental validation. Because of its novel construction with one stator and two rotors and the use of compound current, the Super Motor is characterized by higher power density than previous motors. Owing to its increased heat generation density compared with conventional motors, the thermal design was one of the important factors in the development of the Super Motor. Since the Super Motor is built with two rotors on the inside and outside of the stator, it is logical to place the cooling system in between the stator teeth. Electromagnetic field and heat transfer simulations were used to achieve better power performance and cooling performance with this new structure. Experimental results made clear the thermal characteristics of the Super Motor and showed that the required motor performance was achieved.

Keywords : Electric vehicle, Fuel cell vehicle, Hybrid vehicle, Motor, Thermal design

1. Introduction

Hybrid electric vehicles (HEVs) and fuel cell vehicles (FCVs), characterized by their low fuel consumption and low emissions, have attracted a great deal of interest in recent years amid the various discussions prompted by heightened awareness of environmental issues such as global warming. We have conceptualized, researched and developed a high-efficiency, compact coaxial motor called the Super Motor, which is built with one stator and two rotors and can be applied to HEVs and FCVs⁽¹⁾⁻⁽⁴⁾.

This paper describes a simplified model of the Super Motor used in a torque analysis, the cooling system design and detailed thermal characteristics of this uniquely constructed motor. A prototype motor was subjected to analysis and experimentation, and it was confirmed that the predicted and measured results were in good agreement and that the motor was thermally feasible.

2. Overview of Super Motor

Fig. 1 shows a cut-away model of the Super Motor. Built with a rotor on both the inside and outside of its single stator, the Super Motor can output power through two shafts under the application of compound current. In order to drive these dual rotors with a single stator, there must not be any torque interference between the rotors. To accomplish that, magnets having different numbers of pole pairs are used for the inner rotor and the outer rotor. By applying compound current, drive torque is produced only

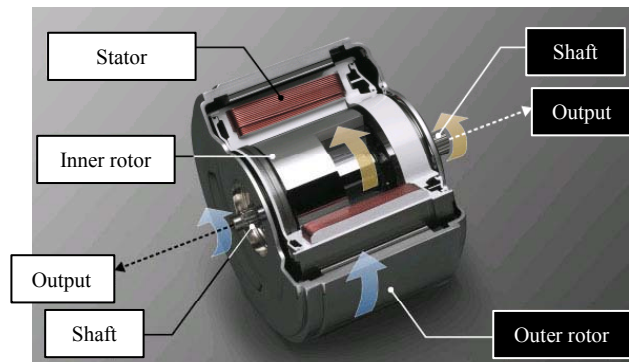


Fig. 1. Cut-away model of Super Motor.

to the extent of the current equal to the number of magnet pole pairs. Correspondingly, the other rotor produces drive torque partially, but the torque is completely cancelled by one revolution of the motor. Hence, the rotor cannot be driven. Because of this mechanism, it is possible to design the motor without any torque interference between the rotors by varying the number of magnetic poles of each rotor.

Fig. 2 shows an example of a series HEV system configuration. This system illustrates one application of the Super Motor, featuring coaxial rotors and shared use of the magnetic circuit and stator coils to achieve a compact, innovative two-motor configuration comprising a generator and a motor. This coaxial design facilitates direct energy exchanges in the form of magnetic flux flow from the generator to the motor, which reduces the amount of power supplied to the motor from the outside. The aim of this design is to reduce the conversion losses of the switching devices and the battery. Consequently, the Super Motor system can achieve dramatic improvements in compactness and efficiency compared with ordinary systems that use two

* NISSAN MOTOR CO., LTD. n-tan@mail.nissan.co.jp
m-arimitsu@mail.nissan.co.jp
y-naruse@mail.nissan.co.jp
j-watanabe@mail.nissan.co.jp

1, Natsushima-cho, Yokosuka-shi, Kanagawa 237-8523, JAPAN

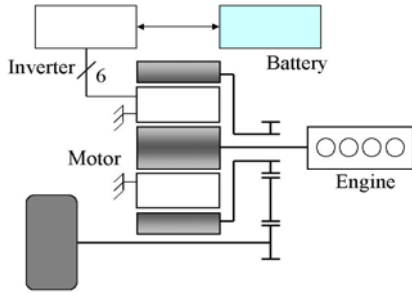


Fig. 2. Configuration of series HEV system.

motors.

3. Simplified Analysis Model⁽⁵⁾

Figure 3 is the simplified model of the Super Motor used in the torque analysis. The following conditions are assumed.

- (1) Two-phase machine model.
- (2) The inner rotor has one pole pair, and the outer rotor has two pole pairs.
- (3) The stator windings for the inner rotor and the outer rotor are indicated separately in Fig. 3, but in actuality they are the same windings in the slots.
- (4) No loss is assumed, and all kinds of non-linear effects are ignored.
- (5) The rotor torque T is calculated with the following equation,

$$T = \frac{\partial}{\partial \theta} W'_m \dots \dots \dots (1)$$

where θ is the rotor position and W'_m is the total magnetic co-energy. Therefore, the inner rotor torque T_i and the outer rotor torque T_o can be expressed as follows by an abbreviated calculation:

$$T_i = \phi_i I_i \sin \delta_i \dots \dots \dots (2)$$

$$T_o = 2\phi_o I_o \sin \delta_o \dots \dots \dots (3)$$

where (ϕ_i, ϕ_o) , (I_i, I_o) , and (δ_i, δ_o) are the magnetic flux, winding current, and the position difference between the electrical and mechanical angles of the inner and outer rotors, respectively. This analysis can also be applied to other motors having a pole pair ratio of $I : N$ ($N \neq I$).

4. Construction of Super Motor

4.1 Mechanical construction The support structure of the Super Motor is shown in Fig. 4. The front side of the stator and the rear side of the outer rotor are secured to the motor case. The outer rotor is supported by the stator and motor case by means of a bearing. Likewise, the inner rotor is also supported, by means of a bearing, by the stator and the outer rotor. In addition, the stator adopts a divided stator

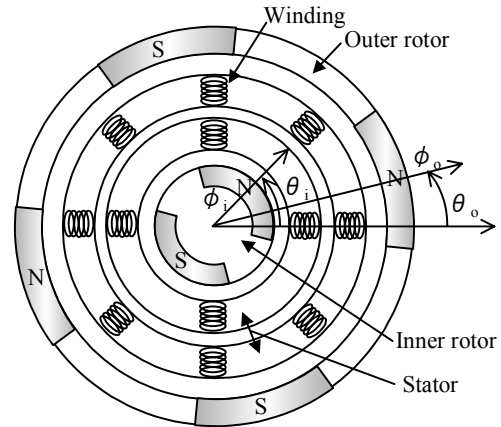


Fig. 3. Simplified model of Super Motor.

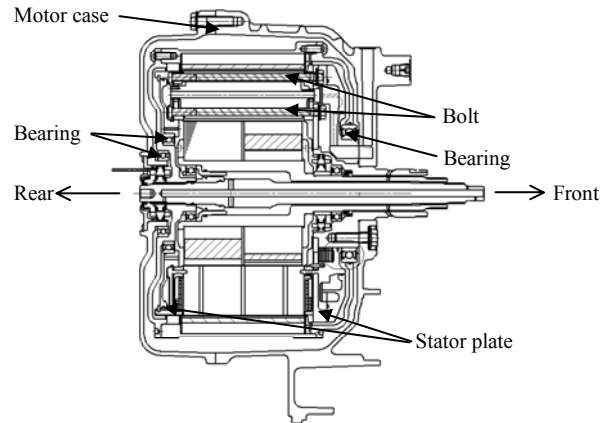


Fig. 4. Super Motor.

core that is sustained by a resin molding and the force of the front and rear stator plates which sandwich the core and make use of the axial force of the bolts. Because the inner and outer surfaces of the stator are covered by the rotors, the places where the stator is attached to the motor case are used for the wiring of the resolver and other components and for the coolant inflow and outflow passages.

4.2 Construction of cooling system The structure of the coolant passages is explained here in reference to Fig. 5. Because rotors are positioned on the inside and outside of the stator of the Super Motor, it is difficult to cool the stator by means of conventional motor case water jackets. Accordingly, it was necessary to construct the cooling system between the stator teeth. Two circular ring-shaped cooling chambers are positioned at the front side of the stator. Coolant flows through inter-coil passages connected in parallel to cool the stator and is then introduced into the rear side. Two inter-coil passages form one pair. The coolant turns around on the rear side and flows through another nine inter-coil passages to the front side again and is then evacuated from the stator. In addition to using long-life coolant (LLC) for cooling, automatic transmission fluid (ATF) is introduced into the gap between the stator and the rotors to provide a parallel cooling effect without any significant increase in friction due to the ATF viscosity.

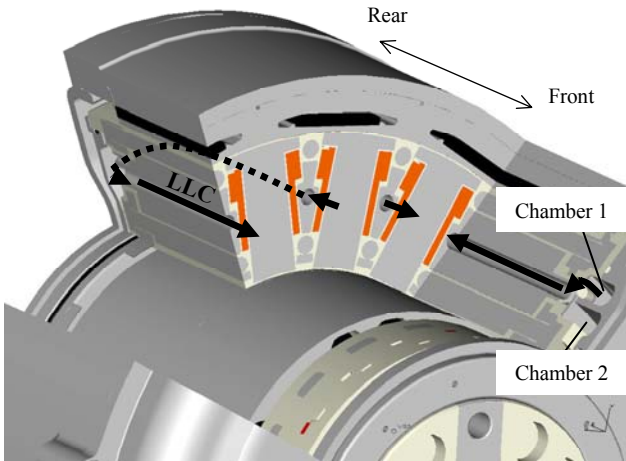


Fig. 5. Cooling system of Super Motor.

4.3 Motor Specifications The specifications of the Super Motor are given in Table 1. Fig. 6 shows a map of the motor efficiency measured experimentally, excluding the mechanical losses when the outer rotor was driven. As this map indicates, the Super Motor achieves efficiency above 96%.

Table 1. Specifications of Super Motor.

Items	Values	Units
Stack length	100	mm
Outer diameter of outer rotor	240	mm
IGBT maximum current	400	A
DC operating voltage	300	V
Material of magnet	Nd-Fe-B (Divided)	—
Number of stator teeth	18	—
Number of pole pairs	Inner rotor	3
	Outer rotor	6
Maximum torque	Inner rotor	70
	Outer rotor	140
Maximum rotational speed	Inner rotor	12000
	Outer rotor	7500

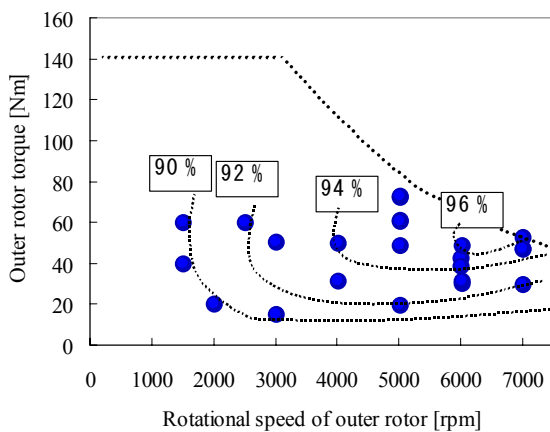


Fig. 6. Efficiency map obtained experimentally.

5. Cooling Performance Design

5.1 Design strategy Because of its novel construction with one stator and two rotors and the use of compound current, the Super Motor is characterized by higher power density than previous motors. Owing to its increased heat generation density compared with conventional motors, the thermal design and thermal countermeasures were important factors in the development of the Super Motor.

Fig. 7 shows plan cross-sectional views of the Super Motor. The stator diameter and teeth geometry were determined on the basis of the electromagnetic field design. A parametric study was conducted to examine the layout of the coils and cooling system in the remaining space between the stator teeth, and an attempt was made to design the copper loss and cooling performance on that basis.

5.2 Thermal-fluid analysis A steady-state heat transfer analysis was conducted in which it was assumed that the LLC coolant flowed through the cooling pipes and the ATF flowed in the gap between the stator and the rotors. In order to take account of the influence of the rotation of the rotors, a velocity component was defined at the rotor wall, representing the boundary with the ATF. The ATF flow fields were found and the temperature distribution was calculated, taking into account heat transfer due to the fluid. Actually, the gap was not a single-phase flow of ATF, but a multi-phase flow of air and ATF. To accelerate the development process, the gap was modeled as an ATF flow field instead of computing complicated multi-phase flow fields. That was deemed sufficient for making a rough estimate in the initial stage of the development process. For the boundary between the cooling pipes and the LLC coolant, the heat transfer coefficient was found from the flow rate because of the simple shape of the cylindrical pipes. The heat transfer coefficient was defined as the boundary condition. Physical properties used in the analysis were shown in Table 2.

A transient heat transfer analysis was conducted in addition to a steady-state heat transfer analysis. However, the heat transfer rate at the gaps between the stator and the rotors was replaced by the heat transfer coefficient rather than computing the ATF flow fields. It takes longer than

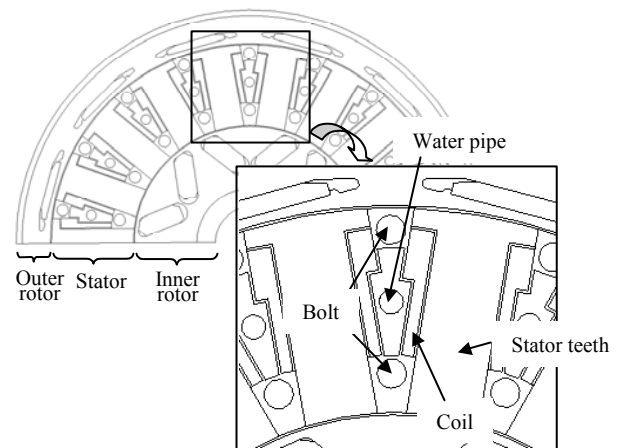


Fig. 7. Stator of Super Motor.

Table 2. Physical properties of materials.

Items	Conductivity [W/mK]	Thermal resistance [m ² K/W]
Teeth	35	-
Coil	390	-
Resin	1.25	-
Bolt	14	-
Insulation sheet	0.138	-
Water pipe	390	-
Magnet	6.5	-
Bond	0.45	-
Shaft	42.3	-
Outer shell	42.3	-
ATF	0.137	-
Coil-Coil	-	0.00025
Metal-Resin	-	0.0000769
Magnet-Bond	-	0.0000357
Core-Shell or Shaft	-	0.0001
Insulation sheet- Coil or Core	-	0.00008

1,000 seconds for the stator to reach a thermally steady state. Accordingly, computing the ATF flow fields as unsteady flow for such a long interval is not a practical way of predicting the temperature of the stator.

5.3 Design of cooling system Assuming a certain motor drive torque, the copper loss was calculated using the number of coil turns and coil shape, i.e., the area occupied by the coils between the stator teeth, as the parameter. The copper loss can be held to a low level by increasing the area occupied by the coils. In other words, the resistance of the copper wires can be reduced by increasing the number of coil turns so as to reduce the current and also by increasing the cross-sectional area of the copper wires. As a result, the copper loss can be kept low under a condition of a certain motor drive torque. However, as a result of doing that, the area that could be allocated for the cooling system would be reduced, giving rise to concern about deterioration of cooling performance.

On the other hand, increasing the area of the cooling system would reduce the area occupied by the coils and necessarily reduce the cross-sectional area of the copper wires. That in turn would require a larger current, causing the copper loss to increase.

The copper loss thus obtained on the basis of this analysis was used to calculate the maximum coil temperature. The maximum coil temperatures, calculated as a function of the area occupied by the coils, are compared in Fig. 8.

When the area occupied by the coils reaches approximately 150 mm², layout constraints exist, for example, with respect to interference between the coils wound on adjacent stator teeth or with the cooling pipes. Since each layout achieves approximately a comparable level of cooling performance near the layout constraints, it was decided to adopt 24 coil turns and a cross-sectional area of 2.2 x 1.3 mm, taking into account the adjustment of tension when winding the coils and the coil deflection, which were technical issues that were encountered in building the prototype motor.

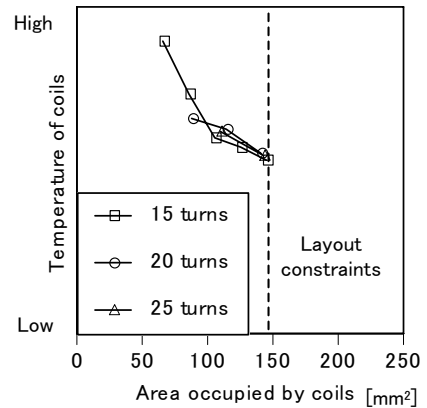


Fig. 8. Comparison of maximum coil temperatures.

6. Results and Discussion

6.1 Steady-state motor temperatures An experiment was conducted to measure the temperature of the prototype motor. Because the purpose of this work was to confirm the cooling performance design, current values were selected that would increase the total loss at operating points where relatively large losses occurred. The loss levels were also determined in an electromagnetic field simulation under the same operating conditions, and the motor temperature distribution was calculated from a thermal-fluid analysis. An example of the calculated temperature distribution and the places where the temperatures are measured are shown in Fig. 9.

The calculated and measured results for the steady-state temperature of the stator are compared in Fig. 10. Above the straight diagonal line in the graph, the calculated temperatures were higher than the measured ones, whereas below the line the measured temperatures were higher than the calculated values. The results confirmed that the thermal-fluid analysis of the motor temperature provided sufficient prediction accuracy for use in designing the motor, although some scatter of the temperature plots is seen which can presumably be attributed to errors in the

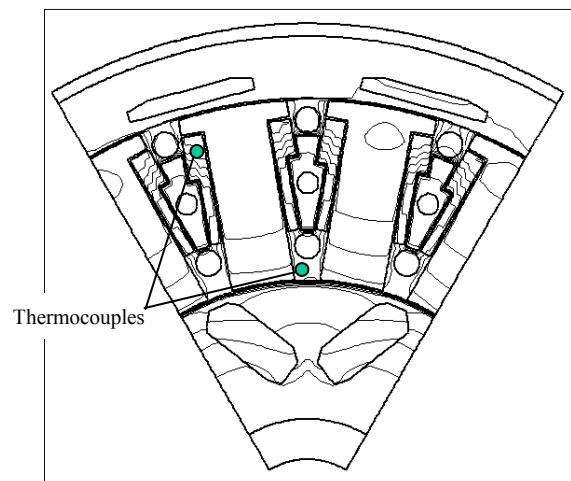


Fig. 9. An example of the calculated temperature distribution.

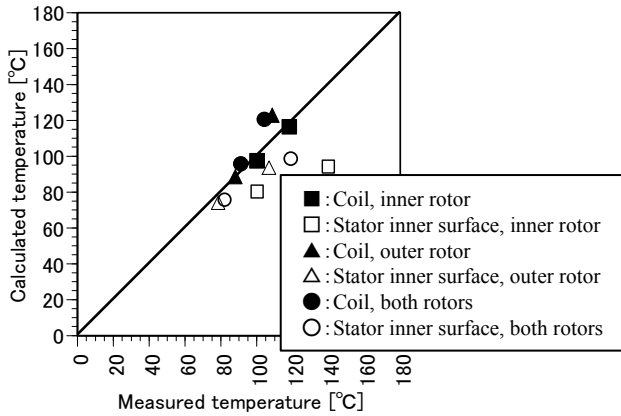


Fig. 10. Comparison of the motor temperatures.

iron loss distribution and heat transfer rate at the gap. The calculated temperatures of the stator inner surface in particular were lower than the measured ones because the gap was modeled as an ATF flow field and the heat transfer rates were calculated higher than those of the actual motor.

The relationship between the total loss and the steady-state maximum temperatures of the coils and stator inner surface was found experimentally and the results are plotted in Figs. 11, 12, and 13. Under the steady-state operating conditions, it was found that the maximum temperature of the motor showed almost a linear relationship with the total motor loss regardless of the operating mode, i.e., operation of either the inner rotor or the outer rotor independently or the combined operation of both rotors. Therefore, motor temperatures for the combined operation of both rotors are not significantly higher than those for independent operation of inner or outer rotor, and thermally special consideration is not necessary for the combined operation of both rotors. However, the slopes of the temperature rise differed for each operating mode, which can be explained in terms of the loss distribution.

Under the steady-state operating conditions where the total loss was 5 kW, the temperatures of the coils and stator inner surface were below 160°C. These results confirmed that the Super Motor did not have any thermal problems as a motor, while achieving maximum efficiency greater than 96%.

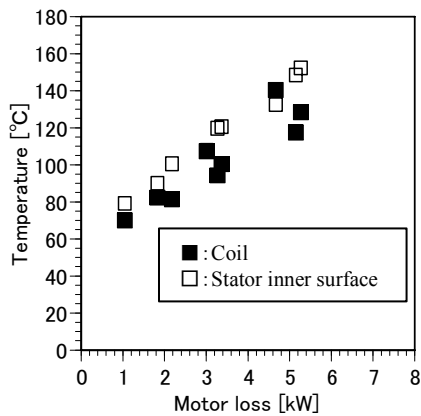


Fig. 11. Measured motor temperatures for independent operation of inner rotor.

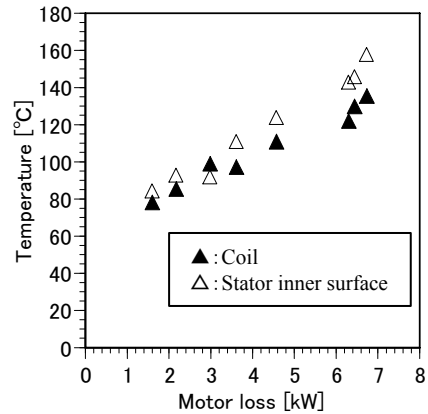


Fig. 12. Measured motor temperatures for independent operation of outer rotor.

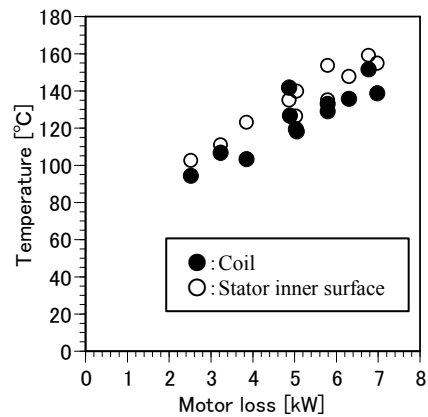


Fig. 13. Measured motor temperatures for combined operation of both rotors.

6.2 Transient motor temperatures The motor design was also validated in a transient heat transfer analysis. The calculated and measured temperatures of the stator are plotted in Fig. 14. The thermal time constant does not vary with the operating conditions if the surrounding environment remains the same. However, the values are not constant as seen in Fig. 14. This is because the physical properties, heat transfer rates at the gap, and heat flux are dependent on the temperatures of the materials, operating modes, and loss distribution, respectively. As mentioned above, the heat transfer rate was defined at the gap, instead of computing ATF flow fields because of computational cost considerations. Fig. 14 shows that the degree of data dispersion for independent operation of the inner rotor was larger than that of independent operation of the outer rotor, which can be explained by the change in the heat transfer rate at the gap. Due to the mechanical construction, the ATF flow at the gap is influenced when the inner rotor is operated, and consequently, the temperature of the motor is affected. An example of temperature rise curves is found in Fig. 15.

The relationship between the total loss and the thermal time constants of the coils and stator interior was found from the experimentally obtained temperature rise curves and plotted in Figs. 16, 17, and 18. The scatter of the thermal time constants, especially for independent

operation of the inner rotor, can be explained by the same reason as in the previous paragraph. It is safe to say that the thermal time constant of the Super Motor is approximately 200 seconds.

The foregoing procedure was used in designing the cooling performance of the Super Motor. A simplified heat transfer simulation was run, and it was verified that the simulation provided reasonable estimates of motor component temperatures. Certain modifications should be made to the temperature-dependent physical properties, heat transfer rates at the gap, and loss distribution, in order to estimate the motor temperatures more accurately.

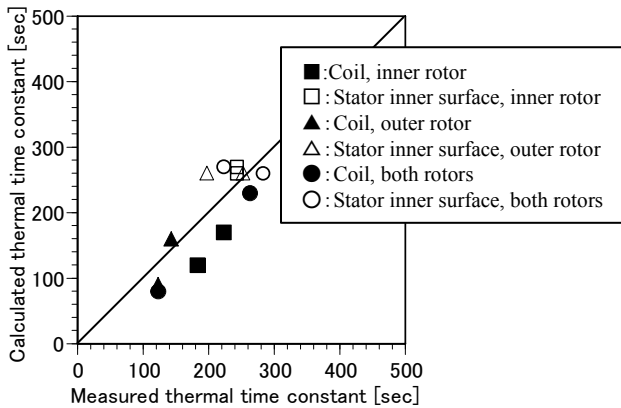


Fig. 14 Comparison of the thermal time constants.

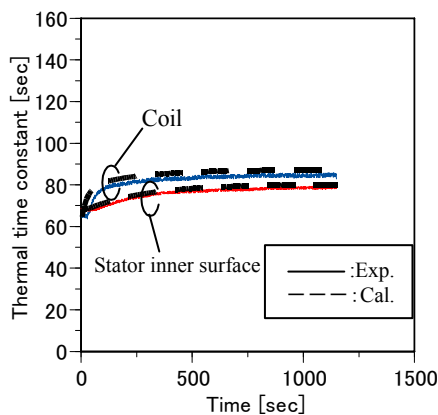


Fig. 15. Comparison of temperature rise curves.

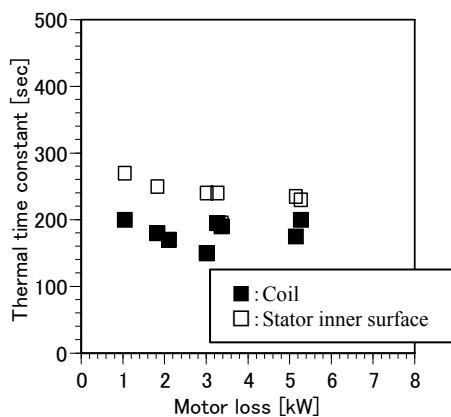


Fig. 16. Thermal time constants for independent operation of inner rotor.

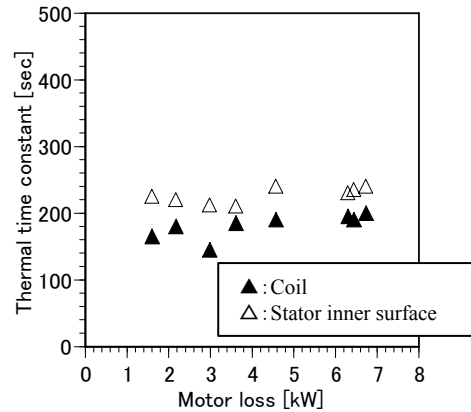


Fig. 17. Thermal time constants for independent operation of outer rotor.

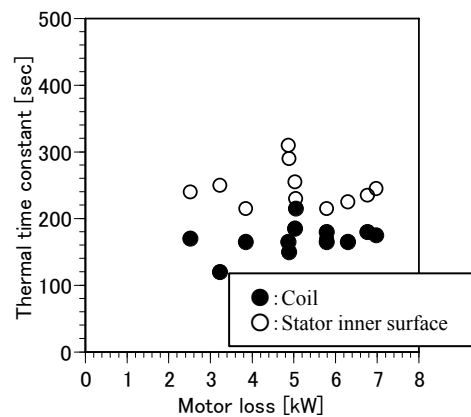


Fig. 18. Thermal time constants for combined operation of both rotors.

7. Conclusions

An effort was made in this work to design the power performance and cooling performance of a motor for automotive use through a series of simulations and experiments. The results obtained are summarized below.

- (1) An effective cooling system was obtained for the Super Motor, which is uniquely built with one stator and two rotors.
- (2) Motor temperatures calculated in a simulation were compared with experimentally measured temperatures. It was confirmed that the simulation provided sufficient accuracy for use in determining the design strategy at the upstream stage of the design process.
- (3) It was validated experimentally that the Super Motor has ample power performance and cooling performance, as intended by the design, while being compact in size.

Acknowledgment

The authors would like to express their appreciation to Yasuyuki Kubota for his valuable assistance and cooperation in connection with the creation of the

simulation models used in this research.

References

- (1) M. Nakano, Y. Minagawa and M. Arimitsu, "New Concept Motor with Multiple Rotors Driven by Compound Multiphase AC," International Power Electronics Conference (IPEC-Tokyo) 2000.
- (2) Y. Minagawa, M. Nakano, M. Arimitsu, H. Furuse and S. Maeda, "Possibility of a Dual Shaft Motor Driven by Compound Current and Its Application to Hybrid Vehicles," Preprint of Autumn 2000 Scientific Lecture Series of JSAE, No. 129 (in Japanese).
- (3) Y. Minagawa, M. Nakano, M. Arimitsu and K. Akatsu, "New Concept Motor with Dual Rotors Driven by Harmonic AC," SAE Paper 2002-01-2857, 2002.
- (4) N. Tan, H. Shimizu, M. Arimitsu, Y. Naruse, J. Watanabe, and M. Nakano, "Development of cooling system for Super Motor," Preprint of Autumn 2004 Scientific Lecture Series of JSAE, No. 60 (in Japanese).
- (5) A. Kawamura, T. Okubora, T. Sugawara, M. Nakano and M. Arimitsu, "Analysis on the Two Axis Motor (Super Motor) for Electric Vehicle," Proceedings of The 8th IEEE International Workshop on Advanced Motion Control 2004, pp.71-74.